Eastern Region Technical Attachment
No. 2012-03
November 2012

Flash Flood Composite Analysis in Vermont and Northern New York

John M. Goff and Gregory A. Hanson*
NOAA/National Weather Service
Burlington, VT

ABSTRACT

A study of 51 flash flood cases in the National Weather Service (NWS) Burlington, Vermont's County Warning Area was conducted. Composite analysis maps were generated, and a subset of 17 available soundings were analyzed. Composite maps showed flash flood-producing storms developed in areas of moderately favorable upper level jet dynamics, weak mid-tropospheric ridging with an approaching short wave trough to the west, a weak surface trough in the vicinity and a low level high moisture axis. The sounding analysis revealed a tall narrow CAPE profile, deep warm coalescence layer, and a light veering wind profile through the boundary layer. Precipitable water, while high, was not extremely anomalous; in most cases only 100% to 150% of normal. The soundings were also marked by a very low Lifted Condensation Level, in many cases below 1,000 feet above ground level. The spatial distribution of reported events suggested evidence of a population bias in northern New York, while this signal was less pronounced in Vermont. Orographical influences were also apparent, especially along the eastern slopes of the Adirondack Mountains. By applying local forecast expertise in conjunction with the parameters identified in this study, it is hoped that skill in detecting the potential for flash flooding in the NWS Burlington, VT county warning area will increase.

**Corresponding author address*: John M. Goff and Gregory A. Hanson, National Weather Service, 1200 Airport Drive, South Burlington VT 05403. E-mail: john.goff@noaa.gov or gregory.hanson@noaa.gov

1. Introduction

Flash flooding is one of the most challenging and hydrometeorological events that the National Weather Service (NWS) Forecast Office in Burlington VT (WFO BTV) faces. Since 1990, 16 of the 28 federally declared disasters in Vermont (Federal Emergency Management Agency 2011) have been for damage caused by flash floods (NOAA 1990-2012). Given the role that flash floods play in disasters, it is critical that the forecaster understand the many complex variables at play during these important events.

General recognition of synoptic patterns, atmospheric thermodynamic properties, topography, previous rainfall, hydrologic factors, land use, radar sampling and beam propagation issues in forecasting and diagnosing flash flooding have all been well documented. The contribution of high humidity, moderate instability, and low shear to excessive rainfall and flash flooding is a common theme in prior literature. Conceptual models for synoptic patterns present in heavy rain and flash flood events form the foundation for heavy rain forecasting (Maddox et al. 1979). The Synoptic, Frontal, and Meso-high archetypes are the basis of pattern recognition for heavy rainfall forecasts.

Chappell (1993) distilled flash flood forecasting to the prediction of rainfall intensity and duration, combined with river basin characteristics. Sounding parameters that would help identify the potential for intense rainfall rates were suggested, and included moderate amounts of convective available potential energy (CAPE) in an elongated vertical distribution, high precipitable water, light to moderate wind shear components, and a highly efficient collision-coalescence process. In a study of heavy rain characteristics in the Eastern Region of the National Weather Service, LaPenta et al. (1995) noted the role of the presence of deep moisture, a nearby surface boundary to focus convection, and light shear in flash flood producing rainfall. Heavy rain in the NWS Eastern Region was "characterized by winds that show marked veering through the lower and middle levels of the troposphere". In earlier work, Chappell (1986) emphasized quasi-stationary convective storms' role in delivering heavy rainfall for a prolonged period of time, and Davis (2001) notes flash flooding resulting from several varieties of convective systems and landfalling tropical cyclones. Differentiating between convective modes allows the forecaster to assess the potential for heavy rainfall duration from single supercell thunderstorms versus training of multicell storms.

Topography, soil type and land use, and antecedent rainfall are all contributing factors in flash flooding. Orographic effects can provide additional lift for heavy rainfall, as well as anchor convective systems over a single location (Davis 2001). Soil moisture, soil type, land use, forest foliation, slope, and basin area determine the amount and force of runoff and its velocity. Rainfall prior to the flash flood producing rainfall can generate runoff and elevate rivers and streams to increase the flash flood potential (Davis 2001; LaPenta et al. 1995; Pontrelli et al. 1999). Although not addressed in this study, these factors are critical considerations for a forecaster evaluating flood or flash flood threats.

This paper will identify and discuss the meteorological parameters contributing to flash flooding in the NWS WFO Burlington VT (BTV) County Warning Area through composite maps and atmospheric sounding analysis. This will lead to a better understanding of these events and enhance awareness of potential flash flood days at the local level. An outline highlighting the methodology in identification of flash flood events is discussed in Section 2. Section 3 will provide analysis of the composite and sounding data, with further discussion on the spatial distribution of flash flood events. Results and concluding remarks are presented in Section 4.

2. Data Collection and Methodology

Fifty one flash flood cases (Table 1) over a 30 year period between 1981 and 2010 were analyzed in the WFO BTV County Warning Area (CWA) to determine primary synoptic weather signatures and sounding profile characteristics typical in such events. The first step in identifying flash flood cases utilized a locally created flash flood climatology database (Breitbach (2009). Breitbach's work compiled 211 flash flood events from NCDC Storm Data for the period 1975 to 2009 in the WFO BTV CWA[1]. In many instances, multiple flash flood events as defined in Storm Data occurred in the same region of the CWA within the same timeframe, and were considered as a single flash flood case. For the purposes of this paper the term "flash flood event" refers to individual NCDC Storm Data records of flash flooding, while the term "flash flood case" is a flash flood that defines a time and location that became a member of the analysis.

The second step was to impose a time separation of one week between flash flood cases to ensure weather systems were discrete. While the practice of separating flash flood cases seems to be generally accepted, there does not appear to be a consensus on the optimal length of time. Cope and Robertson (2007) specified a one day separation, while Jessup and DeGaetano (2008) utilized one week. The goal of temporal separation was to avoid influencing the composite analysis with multiple samples from the same airmass. However it is possible that instilling a temporal separation could introduce another type of bias, such as the elimination of persistent airmasses or weather systems that should have been allowed in the reanalysis. While there were no explicit landfalling tropical systems in the data set, the study does not differentiate systems that may have had tropical origins.

The North American Regional Reanalysis (NARR; Mesinger et al. 2006) 3-hourly data closest to the time of each flash flood case was used to generate hourly spatial composites of numerous synoptic scale meteorological fields to gain a better understanding of the larger meteorological features. A variety of synoptic scale meteorological fields were examined. These included: 1) isotachs at 925, 850, 700, 500 and 250 hPa, 2) geopotential heights at 850 and 500 hPa, 3) specific humidity at 850 and 700 hPa, 4) mean columnar moisture convergence, 5) Lifted Index (LI), surface-based Convective Available Potential Energy (CAPE) and Convective Inhibition (CIN), 6) mean precipitation rate, 7) mean precipitable water (PWAT) and moisture convergence.

Rapid Update Model (RUC) atmospheric soundings were then constructed using *RAwindsonde OBservation Program (RAOB)* software[2].

[1] Due to internal NWS techniques in coding Flood and Flash Flood events in Storm Data, it is possible that the number of Flash Flood events identified in Breitbach may differ from other similar Flash Flood climatologies.

[2] Version 6.1 for Windows, Environmental Research Services, LLC 2011; accessible from http://www.raob.com/.

Data was limited to locally archived RUC BUFKIT data, which was then reformatted for use in the RAOB program. Selection of the location for each sounding was governed by the closest available BUFKIT profile (in time and location) to the observed flash flood case. This limited the total number of cases for the sounding analysis to 17, from 24 July 2003 onward (Table 2). Due to the small size of the sample, soundings were analyzed on an individual basis, with key mesoscale moisture, wind and temperature parameters identified. These parameters included precipitable water (PWAT), wet bulb zero (WBZ) height, warm coalescence depth (WCD), and lifted condensation level (LCL).

To gain a better understanding of the spatial variability in the flash flood event climatology across the BTV CWA, all 211 observed events identified in Breitbach (2009) were plotted geographically. Maps were also created using ArcGIS software to provide insight as to whether population density created an unintended reporting bias across the region.

3. Analysis and Results

a) NARR Analysis

From the isotach analysis, it was evident that coupled mid-to upper level jet dynamics played a more considerable role in providing synoptic scale lift than at corresponding lower levels. While isotach values at 925 hPa and 850 hPa were comparatively low and generally less than 6 m s^{-1} (Figs. 1 and 2), higher values of 10-11 m s^{-1} were found at 500 hPa and 20-22 m s^{-1} at 250 hPa. The coupled left exit and right entrance regions of the 500-hPa and 250-hPa jet features was found to be more significant in enhancing synoptic scale lift (Figs. 3 and 4). These findings support prior research showing that many heavy precipitation episodes in the northeastern U.S. are characterized by light flow in the lower troposphere, and moderate flow at mid and upper levels (Harnack et al. 2001). This tends to foster slower storm cell movement (Jessup and Degaetano 2008) while promoting a mechanism for sustained updrafts through the convective column.

Analysis of 850-hPa and 500-hPa atmospheric height fields also supports prior research (Cope and Robertson 2007) by showing broad troughing across the northeastern states under low amplitude cyclonic flow (Figs. 5 and 6). The 850-hPa trough was slightly deeper and more amplified than its counterpart at 500 hPa across the BTV CWA, and appeared to play a stronger role in determining the likelihood of flash flooding due to greater moisture convergence and transport.

Perhaps the most valuable indicators for flash flooding from a synoptic scale perspective are those associated with moisture and moisture convergence. The axis of highest NARR mean columnar moisture convergence extended from the Hudson Valley of New York northeastward across most of central and northern New England (Fig. 7). The maximum values occur across the central and northern portions of Vermont and New Hampshire where values in excess of 1 kg m^{-2} are evident. This signature of higher columnar moisture convergence has been previously identified in a local study performed on a single flash flood case in Addison County, VT (Hanson 2004). Additionally, plots of precipitable water (PWAT) show an axis of values in the 35-40 mm range extending from the coastal Mid-Atlantic States north into eastern New York and New England (Fig. 8). These are above the normal median values expected for the BTV CWA during

June, July and August based on NWS Albany NY RAOB climatology values near 30 mm (National Weather Service 2011). Additionally, the axis of maximum PWAT values is clearly oriented south to north across the BTV CWA in the composite analysis indicating at least the potential of heavier rainfall in this region should other favorable factors exist. Plots of 850-hPa and 700-hPa specific humidity show an almost identical signature with an axis of higher values also aligned south to north from the Mid-Atlantic States into New England (Figs. 9 and 10). Finally the NARR composite mean precipitation rates (Fig. 11) showed a clear maximum area over eastern New York through Vermont into northern New Hampshire. Values of 1.8×10^{-4} kg m^{-2} s^{-1} were noted in this area with maximum values across Vermont in excess of 3.6×10^{-4} kg m^{-2} s^{-1}.

Additionally, several atmospheric stability parameters were analyzed including CAPE, lifted index (LI) and convective inhibition (CIN). Figure 12 shows a modest CAPE axis extending north and east into eastern New York and New England with values ranging from 500-800 J kg^{-1}. LI values show a similar pattern with an axis of values ranging from -1 to -2 extending north and east across the BTV CWA (Fig. 13). Figure 14 shows low convective inhibition near -10 J kg^{-1} across the study region. These findings are similar to those of Chappell (1993) which showed that during many flash floods the atmosphere is characterized by only modest buoyancy in the boundary layer such that moist parcels remain in the storm updraft longer and thereby have the potential to produce greater rainfall rates given the presence of deep moisture.

b) RUC Sounding Analysis

1) WIND AND THERMAL STRUCTURE

Atmospheric soundings using the subset of 17 archived RUC model exhibited several key features evident during flash flood cases in the BTV CWA. An example is shown in Figure 15. Wind profiles showed values at or less than 20 knots in the boundary layer, increasing gradually to 40 to 50 knots near the 200 hPa level. This implies a low shear environment such that convective towers and precipitation cores are likely to remain more vertically upright leading to higher rainfall rates. A distinct weak warm-air advection pattern with a veering wind profile was also evident from the surface through 850 hPa. Both of these findings are similar to that documented by LaPenta et al (1995). Additionally, boundary layer lapse rates were conditionally unstable in 15 of the 17 soundings. This is not surprising given the low levels of instability observed in the NARR plots and would suggest the potential of weak updraft strength and efficient collision-coalescence processes in storm cores.

2) DISTRIBUTION ANALYSIS OF KEY SOUNDING PARAMETERS

To better understand the variability and importance of key sounding parameters typically associated with flash flooding, frequency distribution plots were constructed for WBZ height, LCL height, WCD, and PWAT. Of these 4 parameters, the analysis identified LCL height and WCD as being the most important in identifying potential for heavy rainfall for the BTV CWA given other boundary layer and synoptic-scale conditions are present as discussed earlier.

Precipitable water values for each case were compared to the median PWAT value for the month of occurrence at the closest available radiosonde site, Albany, NY (National Weather Service 2011). Box and whisker analysis indicated values ranged from 122 percent to 188 percent of normal, with a median value of 149 percent. The presence of above normal PWAT is consistent with prior studies (Pontrelli 1999; Davis 2001; Jessup & DeGaetano 2008). However, while those studies highlighted PWAT near 150 percent of normal, this research finding of flash flood producing PWAT down to 122 percent of normal suggests lower criteria should be used when evaluating the flash flood threat.

The examination of WBZ heights showed values ranging from a minimum of 3071 m (10,077 ft) AGL to a maximum of 4430 m (14,533 ft) AGL (Fig. 17). These values support the idea that flash flood cases are characterized by a warm and deep cloud layer, giving rise to the high rainfall rates observed in each case. Further analysis shows a non-normal distribution in the WBZ data, with the vast majority of cases between 3048 and 3962 m (10,000 to 13,000 ft) AGL (Fig. 18). This is not completely surprising given higher-end values greater than 3962 m (13,000 ft) AGL are more uncommon given Burlington's more northerly latitude. It is apparent from the 17-member sounding dataset that given other favorable parameters, WBZ values in excess of 10,000 feet AGL are likely needed to ensure warm rain processes fully develop. However, high WBZ values do not in and of themselves signify a potential for flash flooding in the causative sense. It is recommended that the forecaster use WBZ height in conjunction with these other parameters to gain a better understanding of the atmospheric environment and the potential for flash flooding.

Warm coalescence depth (WCD) values were more telling in that all but two cases (88%) were above 3000 m with a median value of 3700 m (Fig. 17). Davis (2004) showed that WCD values of at least 3-4 km are preferable to ensure adequate development of heavy rainfall rates dominated by the collision-coalescence process. Without a deep WCD layer, these processes are inhibited thereby limiting rainfall rates and the subsequent flash flood threat. The analysis suggests that higher WCD values of 3000 m or greater serve as a stronger indicator for the potential of flash flooding than PWAT or WBZ height across the BTV CWA.

Additional insight was gained through distribution analysis of the LCL height (Fig. 19). Examination of the 17 cases showed that all but 2 (88%) exhibited values less than 457 m (1,500 ft) AGL with 12 (71%) having values below 305 m (1,000 ft) AGL. These values indicate a very moist boundary layer, and strongly support prior evidence that low LCL heights in combination with a deep WCD and saturated cloud layer act to inhibit dry air entrainment and the development of moist convective downdrafts, limiting the potential for storm cell propagation. It is plausible that under these conditions slow moving storm cells could track across the elevated terrain of the Green and Adirondack Mountains where steeper slopes would foster rapid runoff and the heightened potential for flash flooding. This may be especially true during cases in which lower to mid-level flow is particularly light.

From these findings and the results from the NARR spatial composite analysis discussed above, two 4-panel Advanced Weather Interactive Processing System (AWIPS) procedures were created and available to BTV forecasters in an effort to provide additional hands-on aids to flash flood forecasting. The first procedure includes the primary sounding parameters of WCD, LCL height, moisture convergence, and PWAT. Geopotential heights and isotachs at 925 hPa, 850 hPa, 500 hPa and 250 hPa are included in the second procedure (Fig. 20).

c) Spatial Distribution of Flash Flood Events

To determine the spatial variability of reported flash flood events in the WFO BTV CWA, all 211 events from 1975 to 2009 in the BTV CWA identified from NWS Storm Data in Breitbach 2009 were plotted. These plots were then compared to both orography and population density (Figs. 21 and 22).

The plots for northern New York were quite conclusive showing both orography (Fig. 21) and population density (Fig. 22) playing a role in the identification of flash flood events. Evident in Figure 21 is a concentration of events along the eastern slopes of the Adirondack Mountains where a discrete upslope component likely aids in an overall higher occurrence of convection in this region. The rather steep slopes of the eastern Adirondack Mountains likely provide a mechanism to either 1) anchor convection to the terrain under light low-level easterly flow regimes, or 2) provide a focus for diurnally driven upslope flow. Indeed, these mechanisms may be the driving factor behind the higher concentration of flash flood events reported in Essex County, NY identified by Breitbach (2009). Figure 22 also shows evidence of population bias across the eastern and northwestern slopes of the Adirondacks and into portions the Saint Lawrence River Valley. In these areas small clusters or bull's-eyes are readily apparent, possibly related to the influence of regional population centers such as the Champlain Valley, and the towns of Lake Placid and Malone in an otherwise rather sparsely inhabited area.

In contrast reported events in Vermont do not seem to be concentrated, instead showing a rather homogeneous distribution across the state during the 35 year period. The case could be made of a slight urban bias near the city of Burlington, a somewhat higher density of cases along roads in the Green Mountains, (most of which follow rivers and streams), and a minimum in the less populous northeastern portion of the state. However, in an overall context these features are more subtle than in northern New York.

From these findings it is plausible to assume the predictability of reported flash flood event locations in New York is somewhat greater than in Vermont in the sense that the higher incidence of flash flooding occurs along the steeper eastern slopes of the Adirondacks where orographical and meteorological factors likely play a stronger role. Additionally, lower population density in the northwestern Adirondacks and flatter terrain in the Saint Lawrence Valley factor more readily in a lower rate of flash flood occurrence and a higher bias toward regional population centers. In Vermont, the higher degree of homogeneity in the flash flood distribution suggests a more complex interaction of meteorological and orographical factors at play. In light of these findings, the predictability of flash flood location in a general sense would seem to be more difficult in Vermont than in New York.

4. Conclusions and Future Work

This study provided valuable insight by identifying key synoptic-scale meteorological fields prevalent during a variety of flash flood cases across the NWS

Burlington County Warning Area. Through the use of NARR reanalysis composites, many of the features identified were similar to those reported in prior research. These included a coupled mid to upper level jet structure at 500 hPa and 250 hPa, the proximity of a mid-level trough and associated axis of high precipitable water, and only modest surface-based instability of 500-800 J kg^{-1}. Also noteworthy was the presence of large-scale columnar moisture convergence in the study region.

Additional perspective was gained through the use of RUC model soundings using a smaller subset of available cases. This method identified additional key parameters favorable for flash flooding in Vermont and northern New York. These included a distinct warm air advection signature in lower to mid-levels with light to modest veering flow at or below 20 knots, and a deep cloud layer with WCD heights in excess of 3.4 km and WBZ heights above 3050 m (10,000 ft) AGL. Despite the deep and warm boundary layer, the modest instability of 500-800 J kg^{-1} illustrated in the NARR analysis suggests only weak updraft strength. Given these values in the presence of light low-to mid-level flow and high WCD and PWAT values, cells would tend to be slow moving and produce heavy rainfall rates. Additional insight was gained through LCL height analysis, where 71% of all cases had values less than 305 m (1,000 ft) AGL. This suggests a higher potential for flash flooding given the presence of other favorable factors, as the low LCL values may foster slow cell movement due to the inhibition of moist downdraft formation. From these findings, two AWIPS procedures were developed to aid local forecasters in assessing the potential for flash flooding in the BTV CWA.

Finally, to determine the spatial variability of reported flash flooding across northern New York and Vermont, all flash flood events identified from 1975 to 2009 were plotted. The New York data showed distinct patterns, with orographic effects quite evident along the eastern slopes of the Adirondack Mountains and a possible population bias across the Adirondacks into the Saint Lawrence Valley. In contrast, the Vermont plot showed considerably more homogeneity, offering less evidence of orographic enhancement or population bias.

While the study did identify several key factors in flash-flood-producing storms in the NWS Burlington County Warning Area the available sounding database was limited. Further compilation of cases to form a more robust dataset and statistical tests for significance would prove valuable for future studies on this topic. In addition, the study did not address the role of antecedent soil moisture in producing flash flooding cited in prior literature as playing a key role during many flash flood episodes.

Acknowledgements

The authors would like to thank Paul Sisson, Science and Operations Officer at the NWS in Burlington, VT for guidance and oversight during this process, and Nathan Foster, Operations Program Leader at the NWS in Burlington for his help in creation of the flash flood distribution maps.

Disclaimer

REFERENCES

Breitbach, M., 2009: Flash flooding climatology (1975-2009) for the WFO Burlington, VT county warning area, *NWS Eastern Region Flash Flood Conference,* Wilkes-Barre, PA, National Weather Service. [Available online at http://www.erh.noaa.gov/bgm/research/ERFFW/posters/breitbach_maureen_ERFFW_poster3.pdf]

Chappell, C. F., 1986: Quasi-stationary convective events. *Mesoscale Meteorology and Forecasting,* P.S. Ray, Ed., Amer. Meteor. Soc., 289-310.

Chappell, C. F., 1993: Dissecting the flash flood forecasting problem. Post-prints, *Third Heavy Precipitation Workshop*, Pittsburgh, PA, National Weather Service, NOAA Tech Memo NWS ER-87, 293-297.

Cope, A. M., and L. R. Robertson, 2007: Composite means and anomalies of meteorological parameters for summertime flash flooding in the National Weather Service Eastern Region. *22nd Conf. on Wea. Anal. And Fcstg.*, Park City, UT, Amer. Meteor. Soc. [Available online at https://ams.confex.com/ams/pdfpapers/124202.pdf.]

Davis, R. S., 2001: Flash flood forecast and detection methods. *Severe Convective Storms, Meteor. Monogr.,* No. 50, Amer. Meteor. Soc., 481-525.

Davis, R. S., 2004: The impact of tropical rainfall rates on flash flood detection. Preprints, *22nd Conference on Severe Local Storms,* Hyannis, MA, Amer. Meteor. Soc. [Available online at http://ams.confex.com/ams/11aram22sls/webprogram/Paper81521.html.]

Federal Emergency Management Agency, cited 2011: Vermont state disaster history. [Available online at http://www.fema.gov/disasters.]

Hanson, G., 2004: 28 August 2004 flash flood in Addison County Vermont. *6th Northeast Regional Operational Workshop,* Albany, NY, National Weather Service.

Harnack, R., K. Apffel, M. Georgescu, and S. Baines, 2001: The determination of observed atmospheric differences between heavy and light precipitation events in New Jersey, USA. *Int. J. Climatol.*, **21,** 1529-1560.

Jessup, S. M., and A. T. DeGaetano, 2008: A statistical comparison of the properties of flash flooding and non-flooding precipitation events in portions of New York and Pennsylvania. *Wea. Forecasting,* **23,** 114-130.

LaPenta, K. D., and Coauthors, 1995: The challenge of forecasting significant rain and flooding throughout the Eastern Region of the National Weather Service. Part I: Characteristics and events. *Wea. Forecasting*, **10,** 78-90.

Maddox, R. A., C. F. Chappell, and L. R. Hoxit, 1979: Synoptic and mesoscale aspects of flash flood events. *Bull. Amer. Meteor. Soc.*, **60,** 115-123.

Mesinger, F., and Coauthors, 2006: North American regional reanalysis. *Bull. Amer. Meteor. Soc.*, **87**, 343-360.

National Weather Service, cited 2011: Precipitable water plots. [Available online at http://www.crh.noaa.gov/unr/?n=pw.]

NOAA, 1990-2012: *Storm Data.* Vols 32-54.

Pontrelli, M. D., G. Bryan, and J. M. Fritsch, 1999: The Madison County, Virginia, flash flood of 27 June 1995. *Wea. Forecasting*, **14,** 384-404.

TABLES AND FIGURES

Table 1. List of 51 flash flood cases used in NARR composite analysis.

DATE	TIME (UTC)	EVENT(S)
8/4/2010	4:00	Ellenburg Depot & Altona, NY
8/21/2009	16:30	Chelsea, VT
7/29/2009	12:22	Blissville, VT
8/6/2008	12:30	Forest Dale, Hancock, Barnet Ctr & Robinson VT
6/28/2008	21:30	Rutland, VT
6/15/2008	1:00	Rutland & Ripton, VT
7/11/2007	19:00	Bethel, Stockbridge & E. Barre
6/12/2007	20:00	Wallingford & E. Clarendon, VT
8/1/2006	9:00	Vermontville & Bloomingdale, NY
6/29/2006	22:40	Bakersfield, VT
5/30/2006	17:35	Schroon Lake, NY
5/20/2006	1:00	Montgomery, VT
9/17/2005	0:45	Gouverneur, Pierrepont, Canton, NY & others
8/29/2005	20:00	Weston, VT
7/17/2005	19:15	Gouverneur, NY
6/29/2005	17:00	Williston, VT
6/16/2005	22:00	Peru, Keeseville, Moriah, Crown Pt., Westport, NY & others
6/9/2005	21:00	Crown Pt., Moriah, NY; Plainfield & Calais, VT
8/28/2004	21:45	Bristol & New Haven, VT
8/12/2004	18:30	Worcester, VT
7/12/2004	22:00	Stowe, Moscow & Canaan, VT
8/13/2003	10:00	East Charleston & Island Pond, VT
8/6/2003	0:00	Jay, Ausable Forks & Peru, NY
7/24/2003	14:45	Goshen, Brandon, Forest Dale & Robinson, VT
6/5/2002	22:46	St. Albans, Enosburg, Richmond & Montgomery, VT
7/31/2000	12:00	Cuttingsville, Shrewsbury, Middletown Springs & Ludlow, VT
7/17/2000	1:00	Randolph, Lincoln, Bristol, Ripton & Chittenden, VT
5/10/2000	19:00	Russell, Potsdam, Canton, NY; Moretown & E. Montpelier, VT
8/24/1998	22:00	Berlin & Waitsfield, VT
8/12/1998	0:00	St. Johnsbury, Westford, St. Albans, VT, Ticonderoga, NY & others
7/16/1998	22:00	Mooers, Ausable Forks, Peru, NY & Hinesburg, VT
6/27/1998	4:00	Dannemora, NY, Waitsfield, Bristol, Rochester & Randolph, VT
6/18/1998	8:00	Cambridge, Jericho, VT; Altona & Willsboro, NY
7/15/1997	6:00	Montgomery, Albany & Hardwick, VT
8/3/1996	22:00	Castleton, VT
7/23/1996	22:00	Plattsburgh, NY
6/12/1996	21:00	Merrill, NY; Chester & E. Montpelier, VT
8/7/1990	5:00	Sharon, VT
7/23/1990	17:00	Unknown

7/4/1990	19:00	Unknown
6/20/1990	22:00	Waterford, VT
8/5/1989	0:00	Unknown
7/10/1989	15:00	Keene, NY
7/30/1988	18:00	Poultney, VT
7/21/1987	4:00	Montpelier & Barre, VT
8/8/1986	19:00	Ryegate, VT
7/29/1986	16:00	Island Pond & others
5/23/1986	22:00	Unknown
8/11/1984	17:00	Burlington, VT
7/6/1984	21:00	Williston, VT (Amtrak derailment)
6/16/1981	21:00	Unknown

Table 2. List of 17 flash flood cases used in sounding analysis.

DATE	TIME USED FOR RUC SOUNDING (UTC)	LOCATION FOR BUFKIT/RAOB SOUNDING
08/04/2010	7:00	Burlington, VT
08/21/2009	19:00	Springfield, VT
07/30/2009	1:00	Rutland, VT
08/06/2008	13:00	Rutland, VT
06/28/2008	21:00	Rutland, VT
07/11/2007	18:00	Montpelier, VT
08/01/2006	10:00	Saranac Lake, NY
07/17/2005	18:00	Ogdensburg, NY
06/29/2005	19:00	Burlington, VT
06/16/2005	22:00	Burlington, VT
06/09/2005	22:00	Burlington, VT
08/28/2004	19:00	Rutland, VT
08/12/2004	19:00	Montpelier, VT
07/13/2004	0:00	Montpelier, VT
08/13/2003	6:00	Jay Peak, VT
08/06/2003	0:00	Saranac Lake, VT
07/24/2003	15:00	Rutland, VT

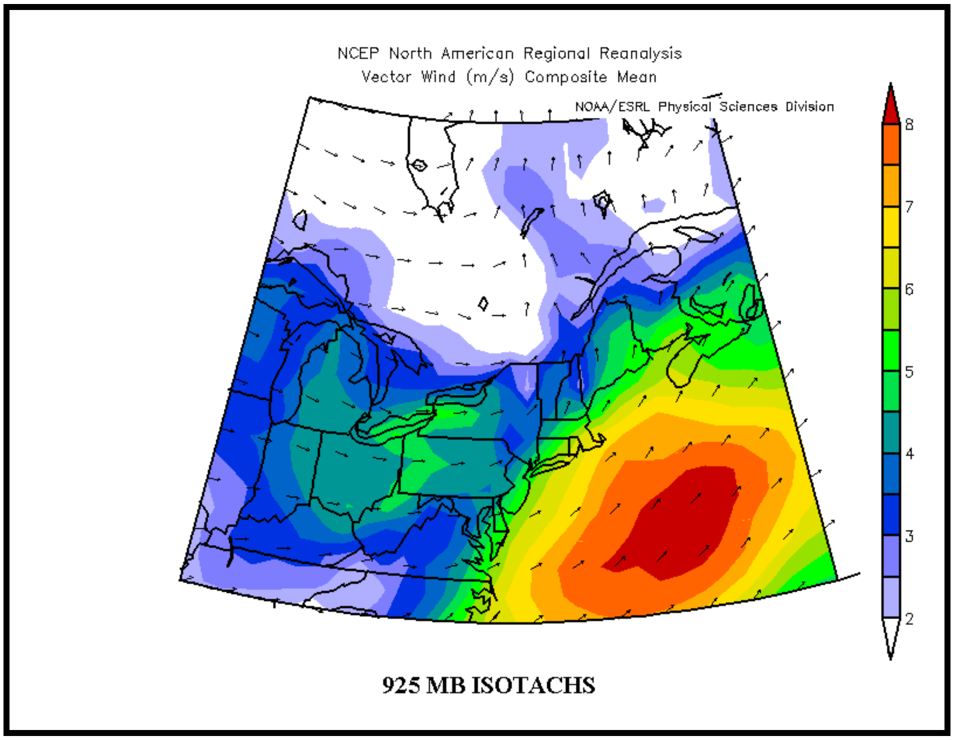

Figure 1. NARR composite mean 925-hPa wind vectors (black arrows) and isotachs (color interval 1 m s^{-1}).

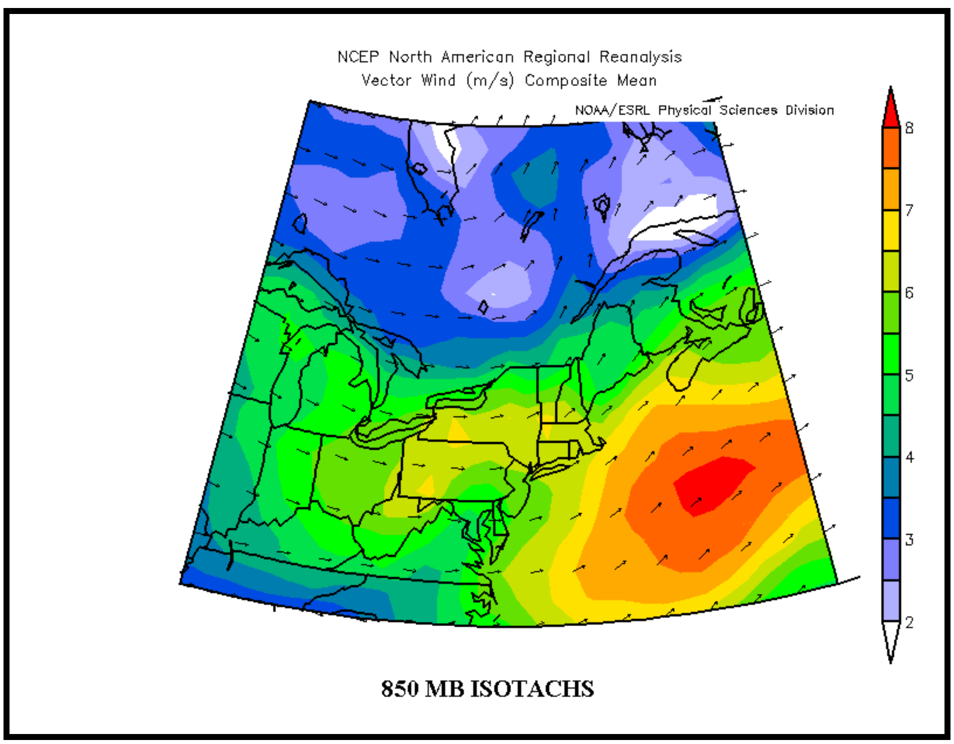

Figure 2. Same as in Figure 1, except for 850-hPa.

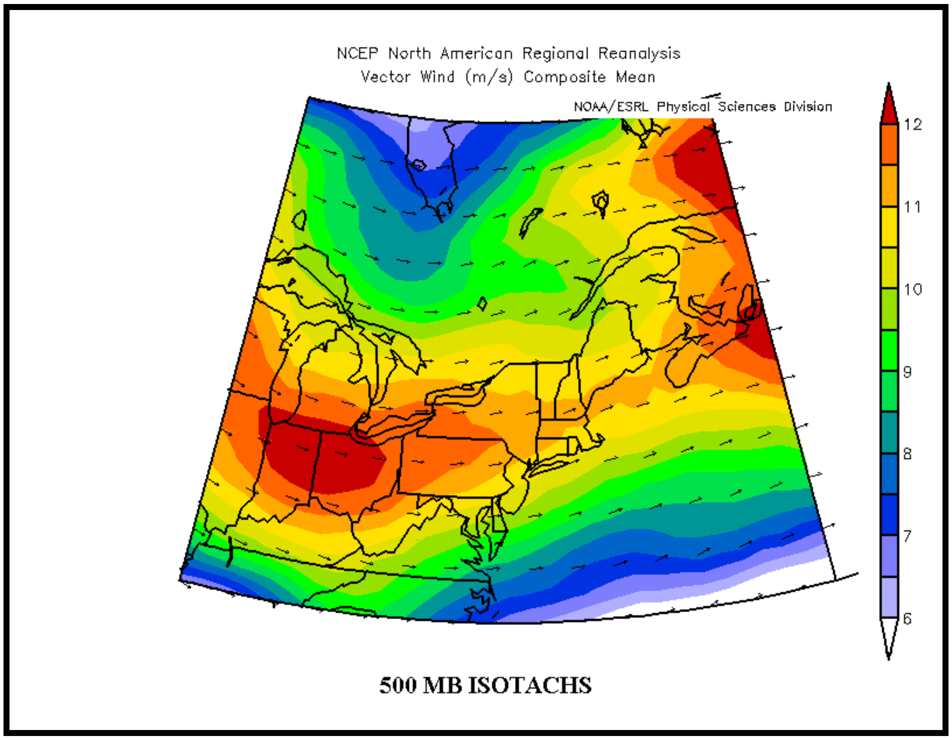

Figure 3. Same as in Figure 1, except for 500-hPa (color interval 0.5 m s^{-1}).

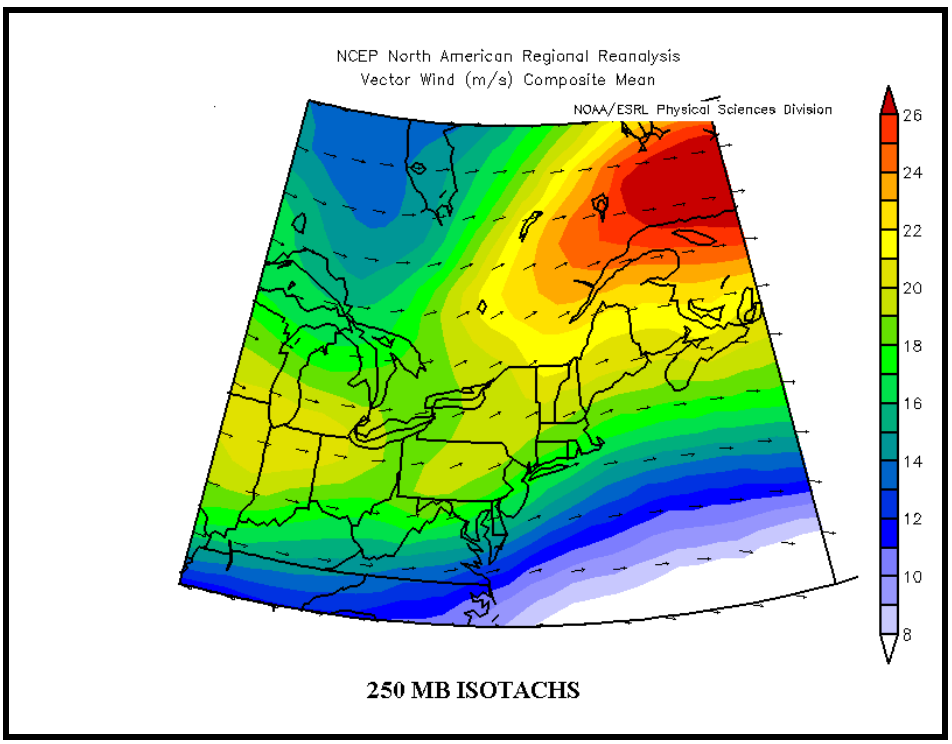

Figure 4. Same as in Figure 1, except for 250-hPa.

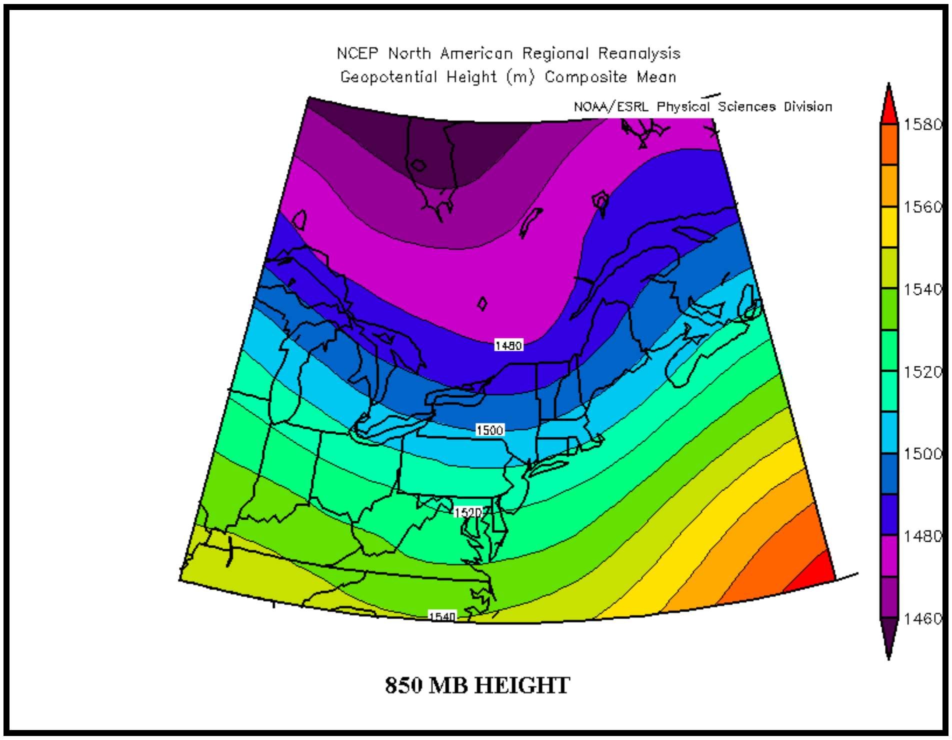

Figure 5. NARR composite mean 850-hPa geopotential height (black lines, shaded; contour interval 10 m).

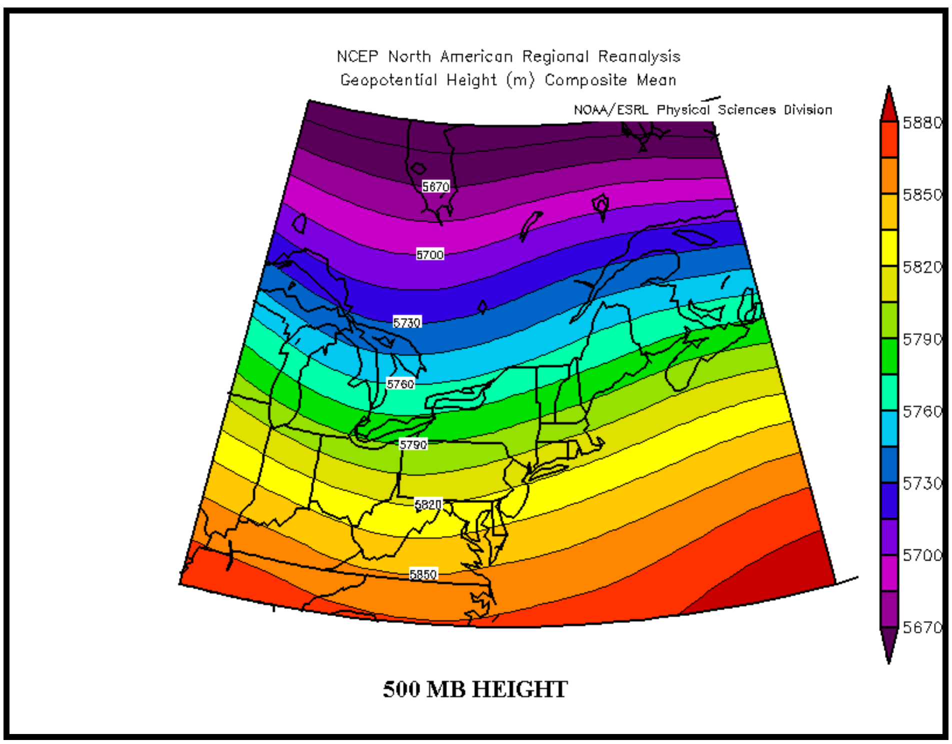

Figure 6. Same as in Figure 5, except for 500-hPa (contour interval 15 m).

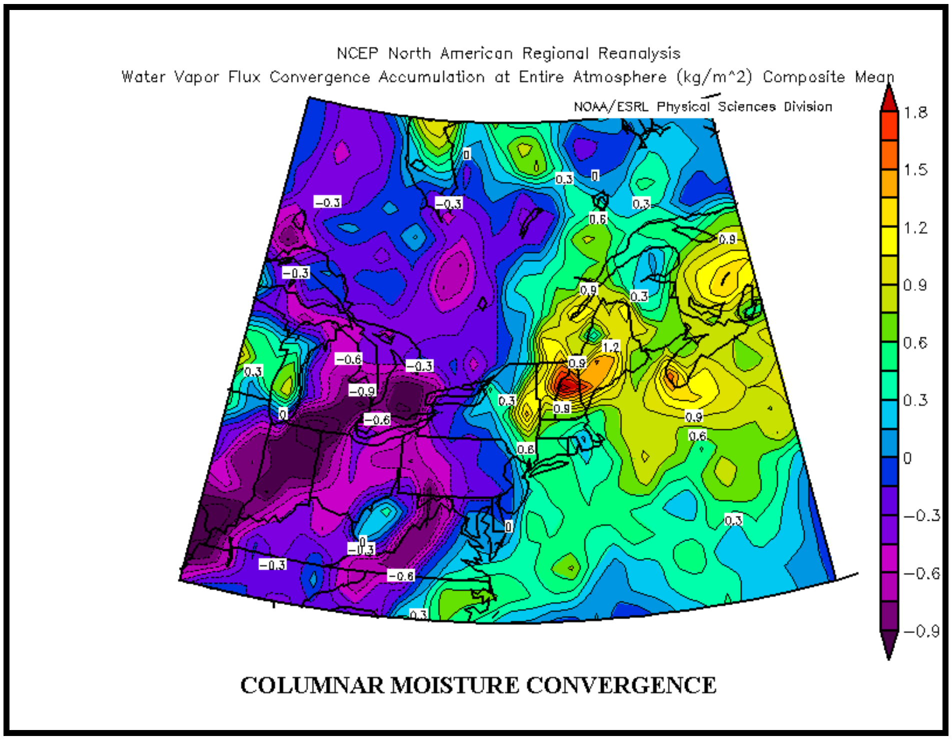

Figure 7. NARR composite mean columnar moisture convergence (black lines, shaded; contour interval 0.15 kg m^{-2}).

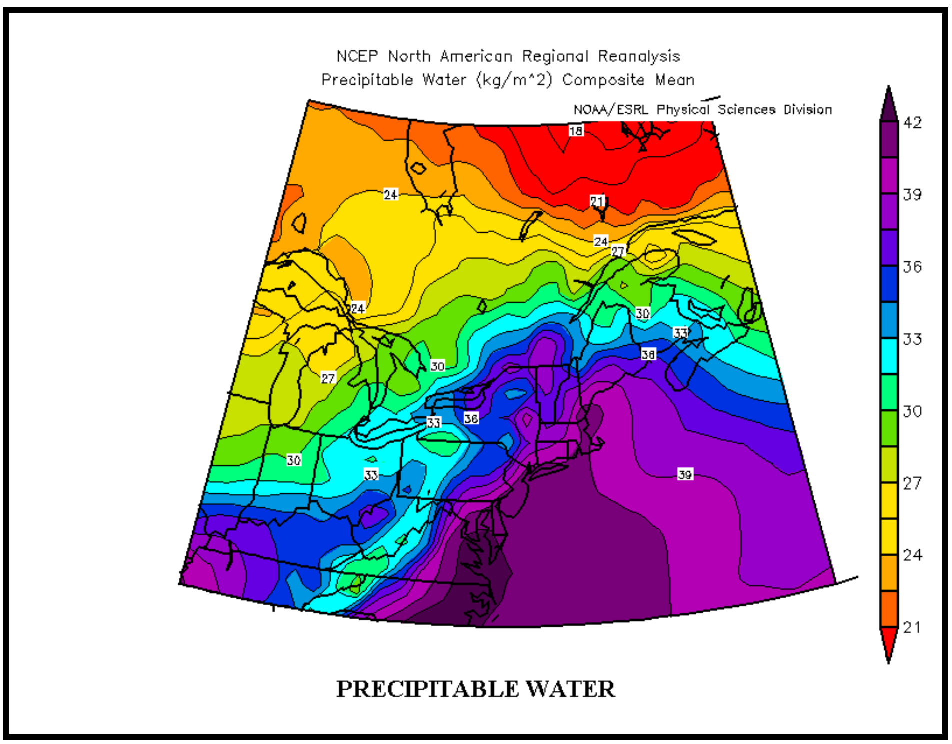

Figure 8. NARR composite mean precipitable water (black lines, shaded; contour interval 1.5 kg m^{-2}).

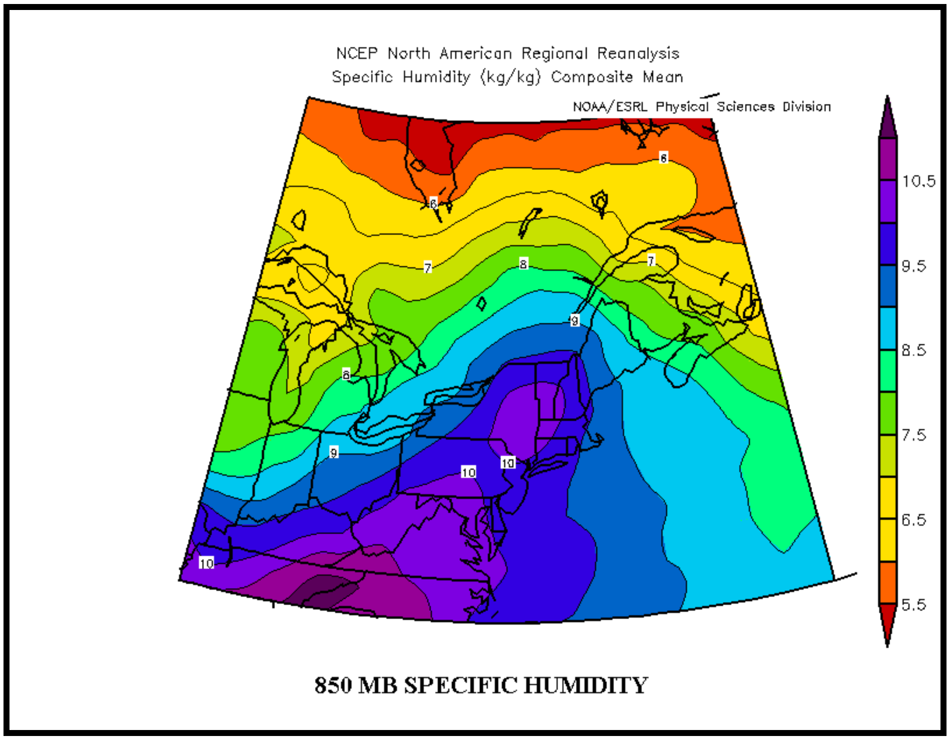

Figure 9. NARR composite mean 850-hPa specific humidity (black lines, shaded; contour interval kg kg^{-1}).

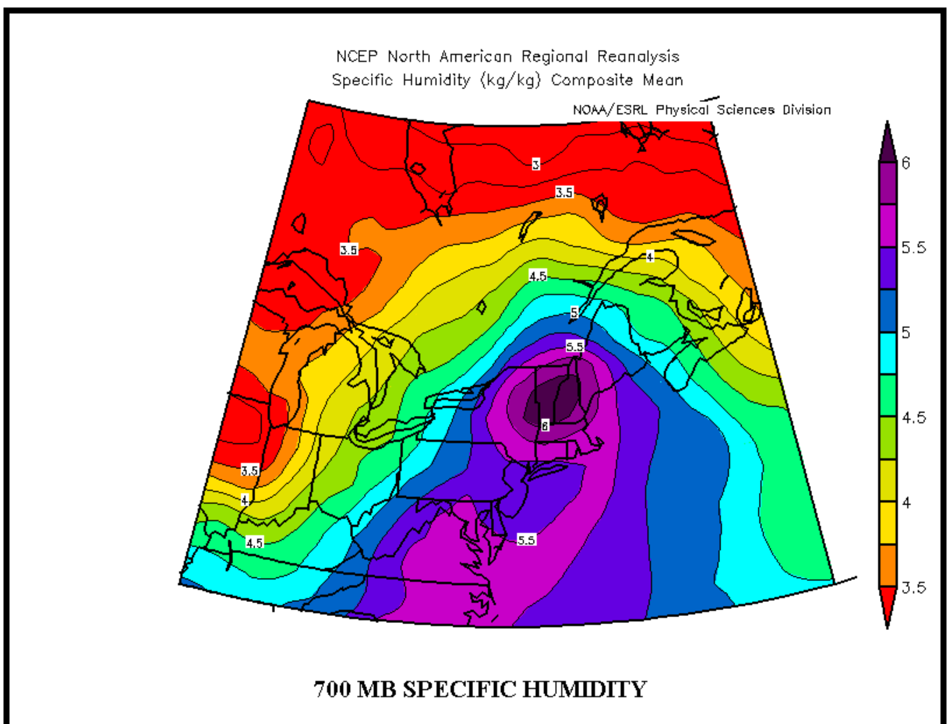

Figure 10. Same as in Figure 9, except for 700-hPa (contour interval 0.25 kg kg^{-1}).

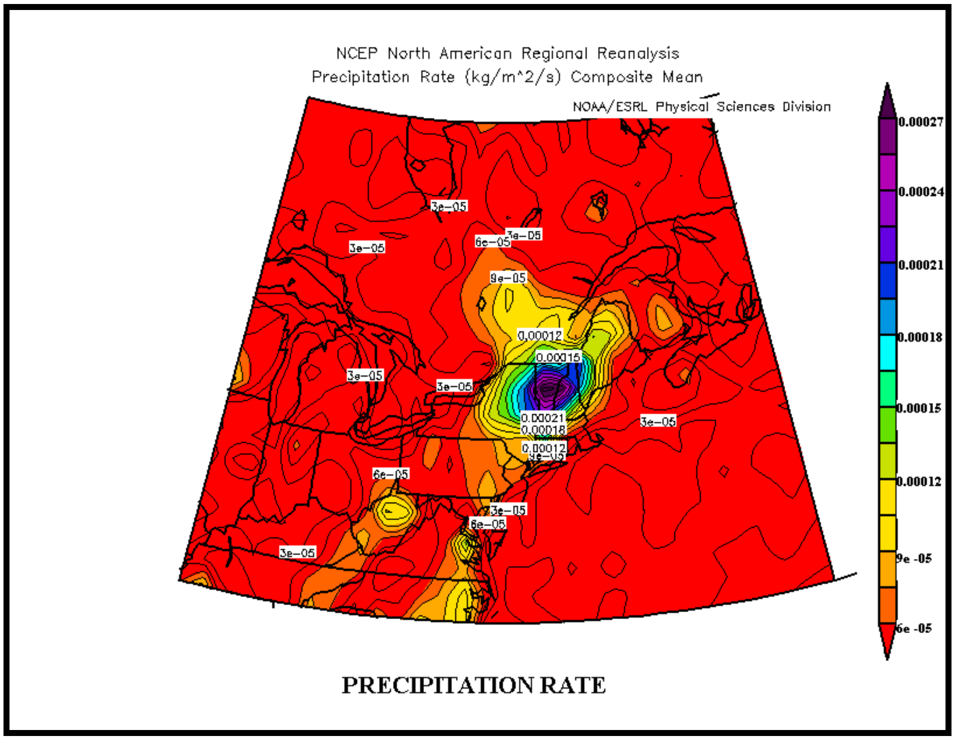

Figure 11. NARR composite mean precipitation rate (black lines, shaded; contour interval 1.5 x 10^{-4} kg m^{-2} s^{-1} (mm s^{-1}).

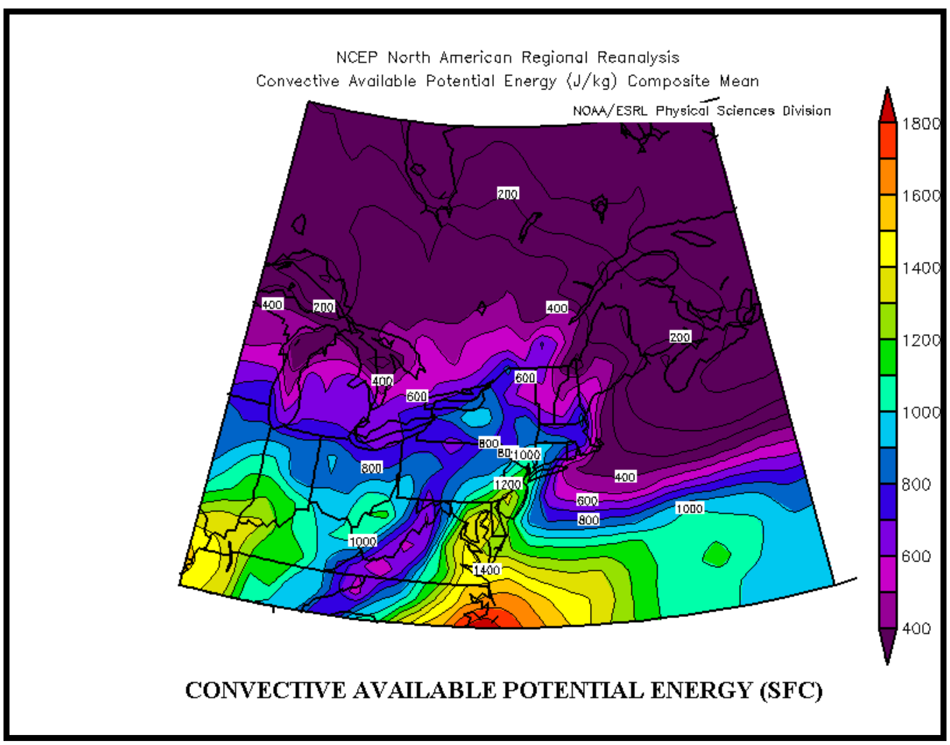

Figure 12. NARR composite mean CAPE (solid lines, shaded; contour interval 100 J kg^{-1}).

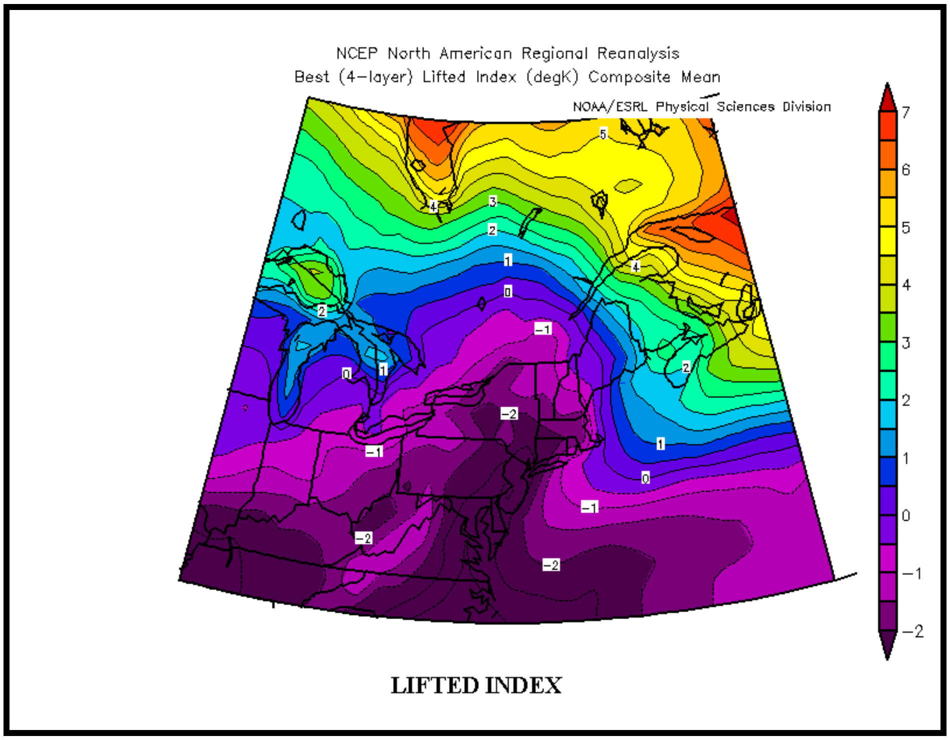

Figure 13. NARR composite mean lifted index (solid lines, shaded; contour interval 0.5 K).

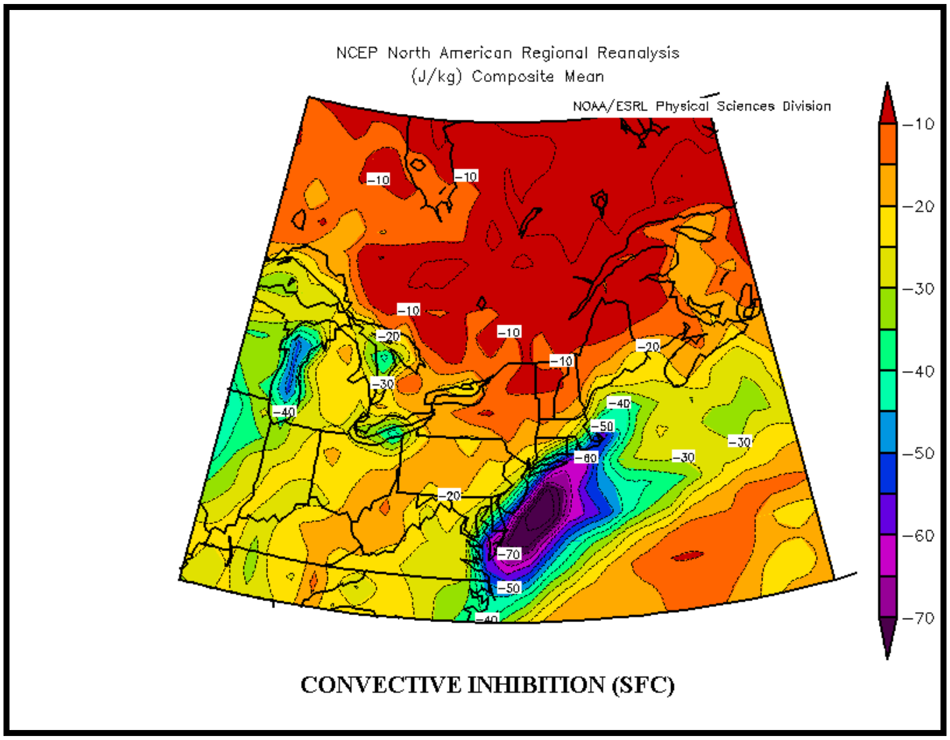

Figure 14. NARR composite mean convective inhibition (solid black lines, shaded; contour interval 5 J kg^{-1}).

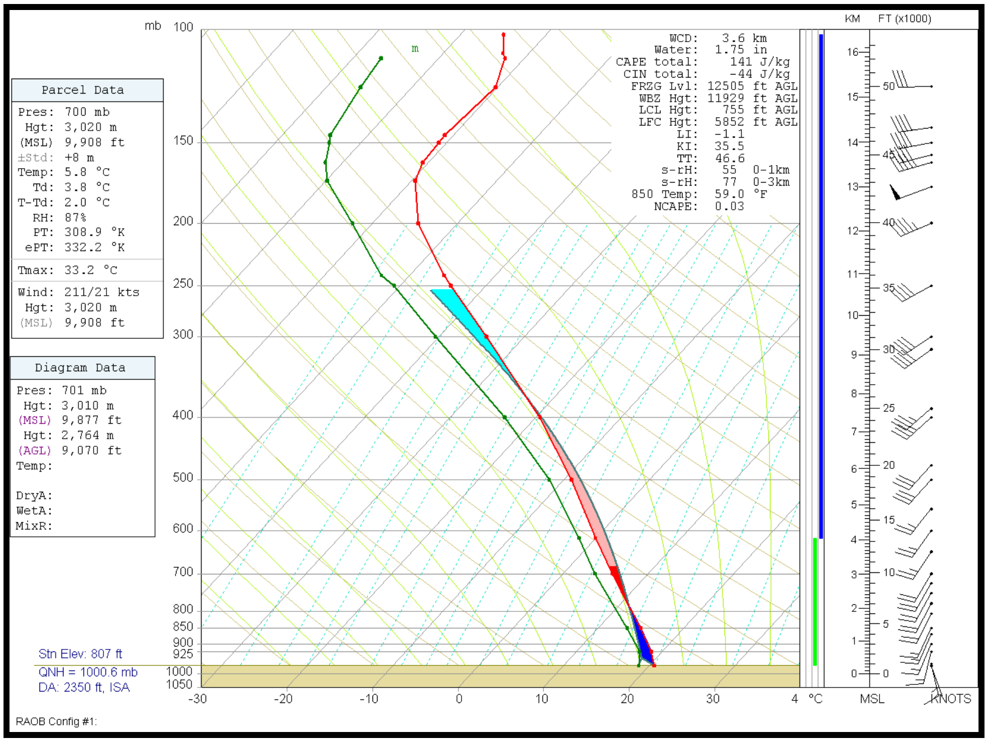

Figure 15. Sample RUC model sounding from the 17-member flash flood subset (CAPE and CIN shaded).

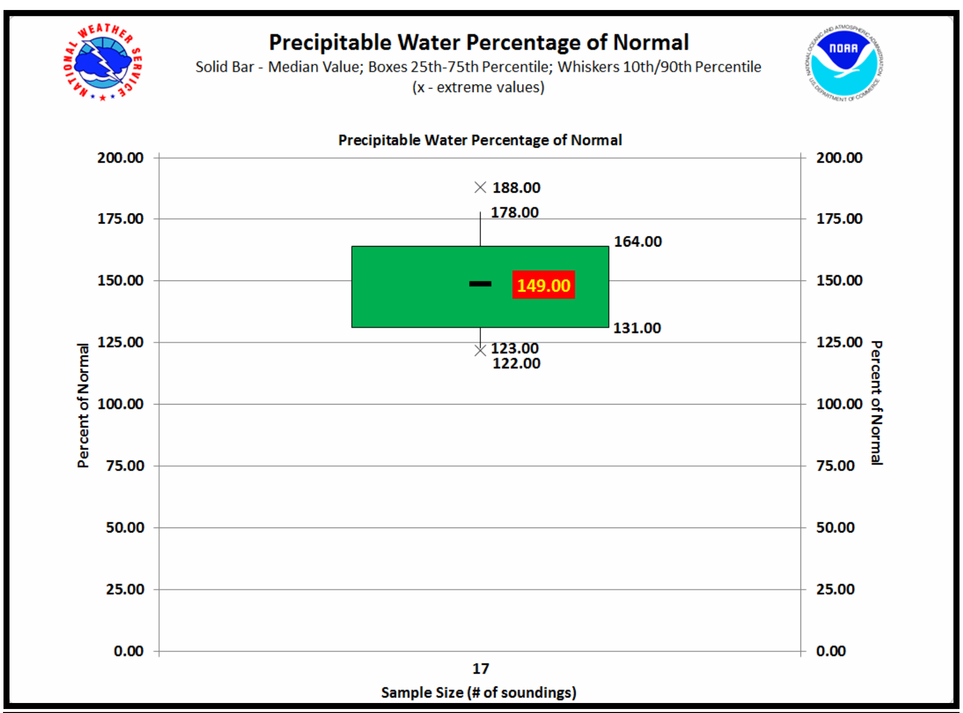

Figure 16. Box and whiskers of precipitable water percent of normal values from the 17-member RUC sounding subset. Values calculated using the ALY summer median value of 30 mm (1.18 in.).

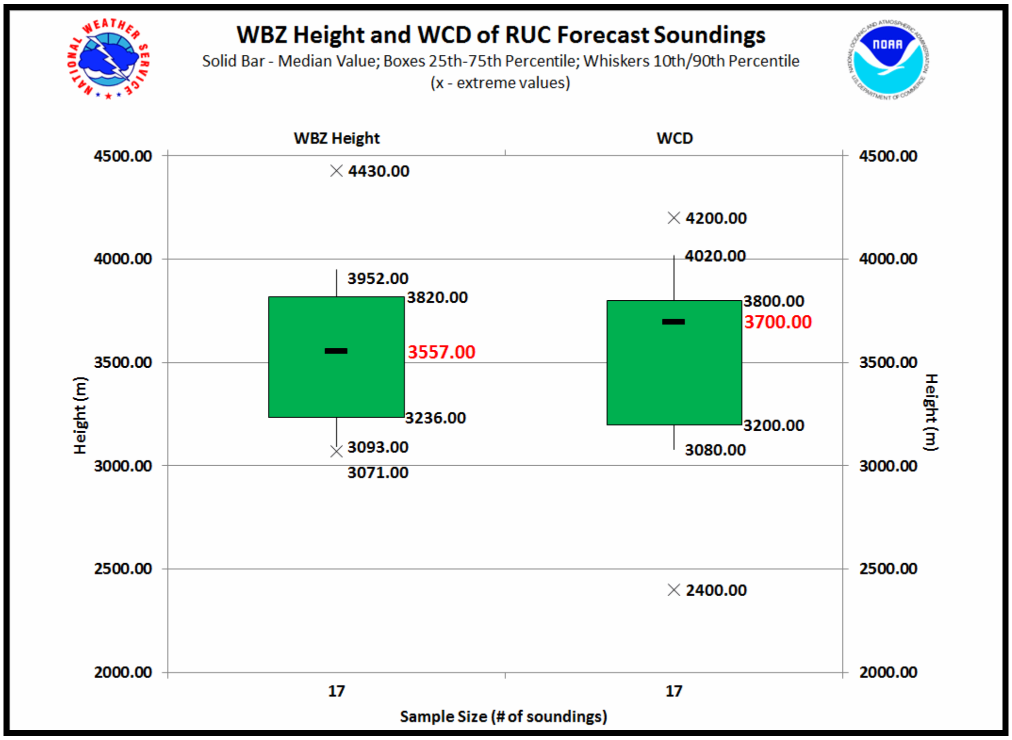

Figure 17. Box and Whiskers plot of wet bulb zero (WBZ) height and warm coalescence depth (WCD) (m) from the RUC sounding subset.

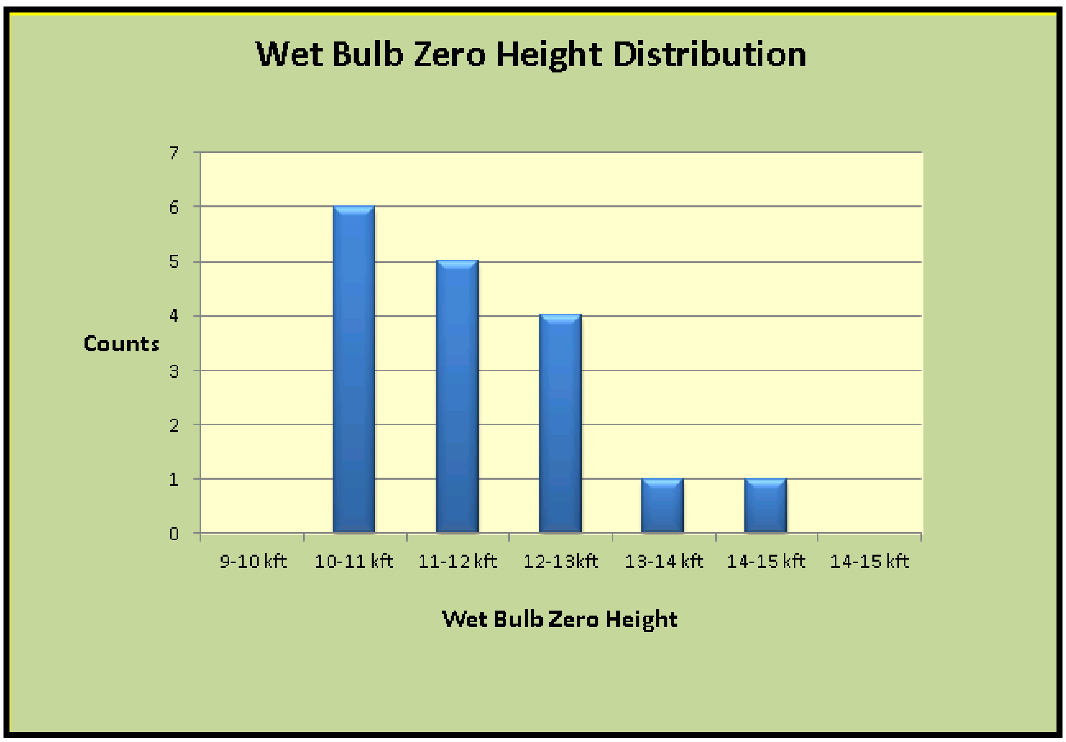

Figure 18. Histogram of wet bulb zero height (kft) distribution from the RUC sounding subset.

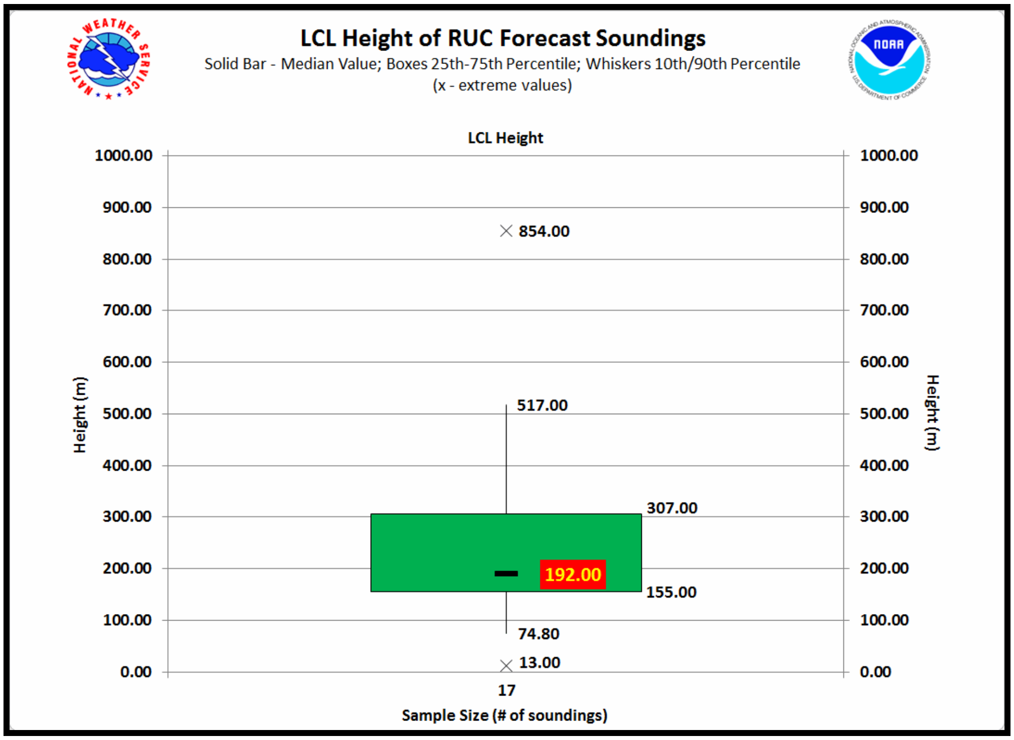

Figure 19. Box and Whiskers plot of Lifted Condensation Level heights (m) from the RUC sounding subset.

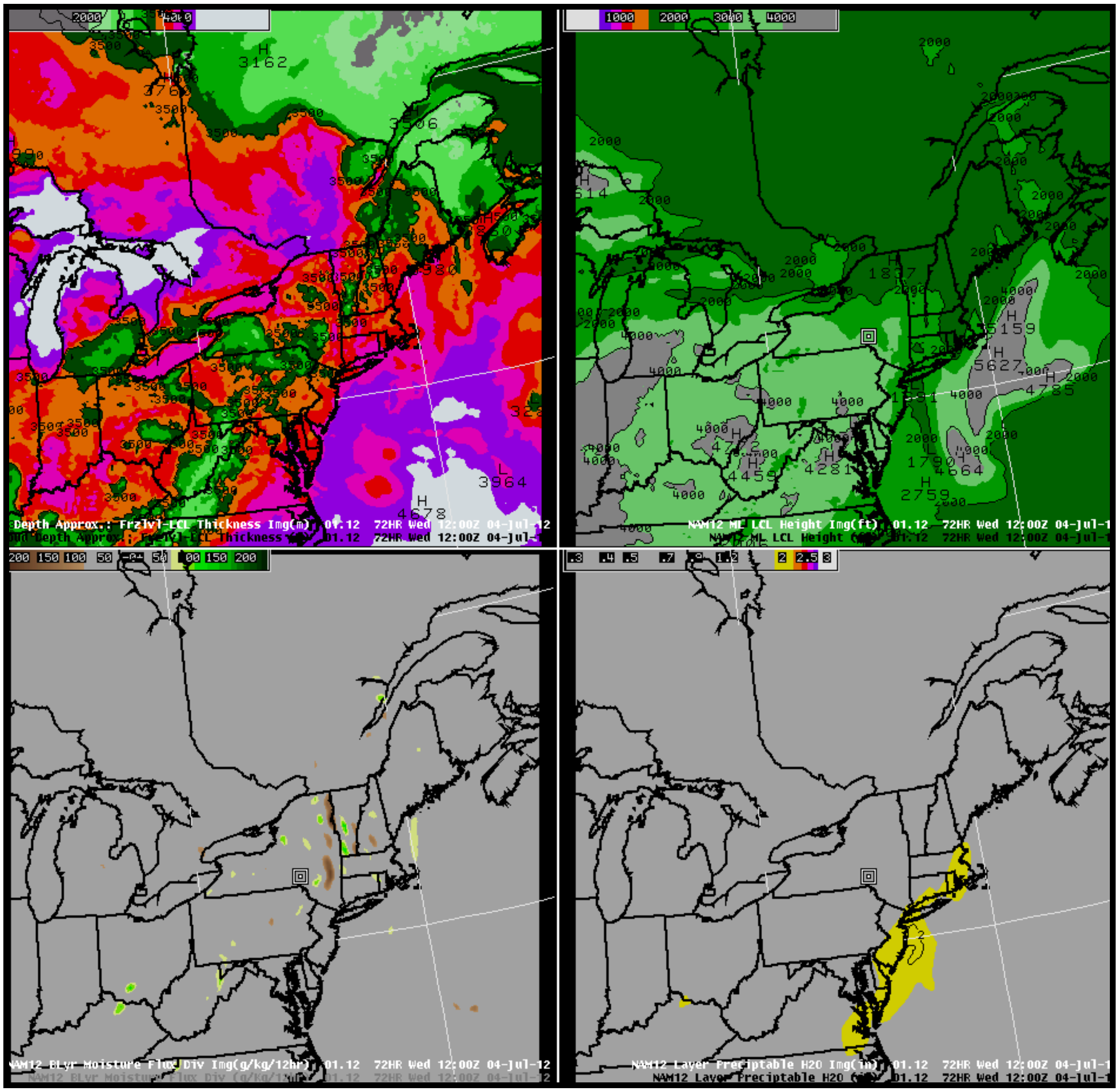

Figure 20. AWIPS 4-panel procedure including (a) Warm Coalescence Depth (m, WCD),(b) Lifted Condensation Level (ft., LCL) Height, (c) boundary layer moisture convergence (gkg^{-1}in 12 hr.;, and (d) Precipitable Water (in., PWAT).

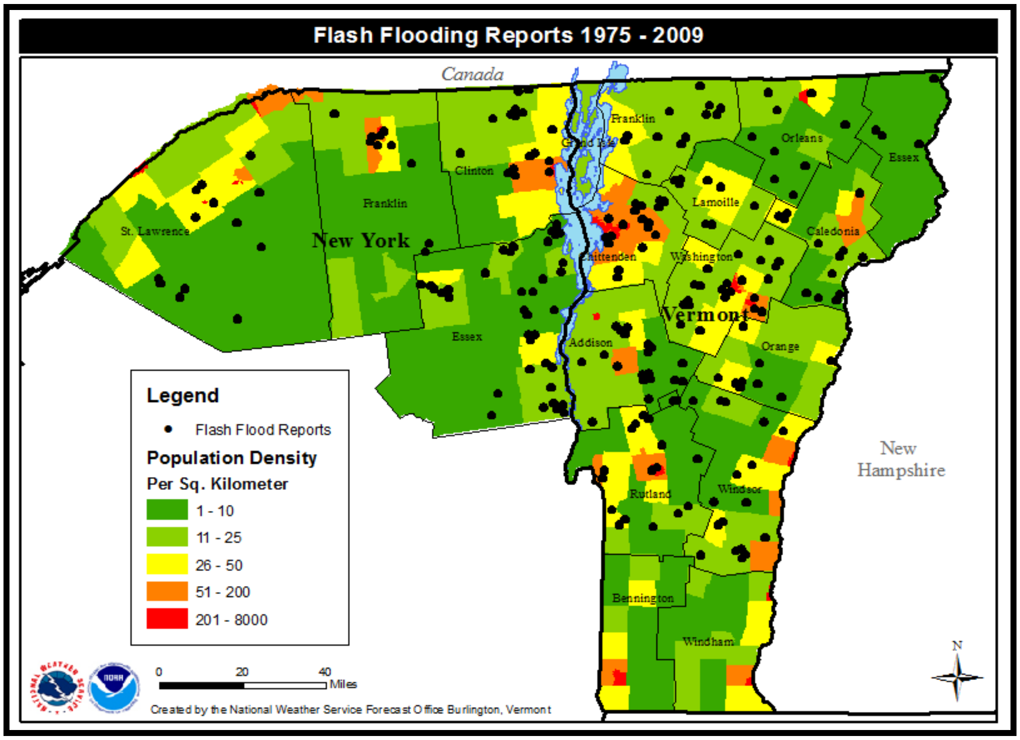

Figure 21. Plot indicating physical location of all documented flash flood events as identified in Breitbach (2009) overlaid atop population density by census tract.

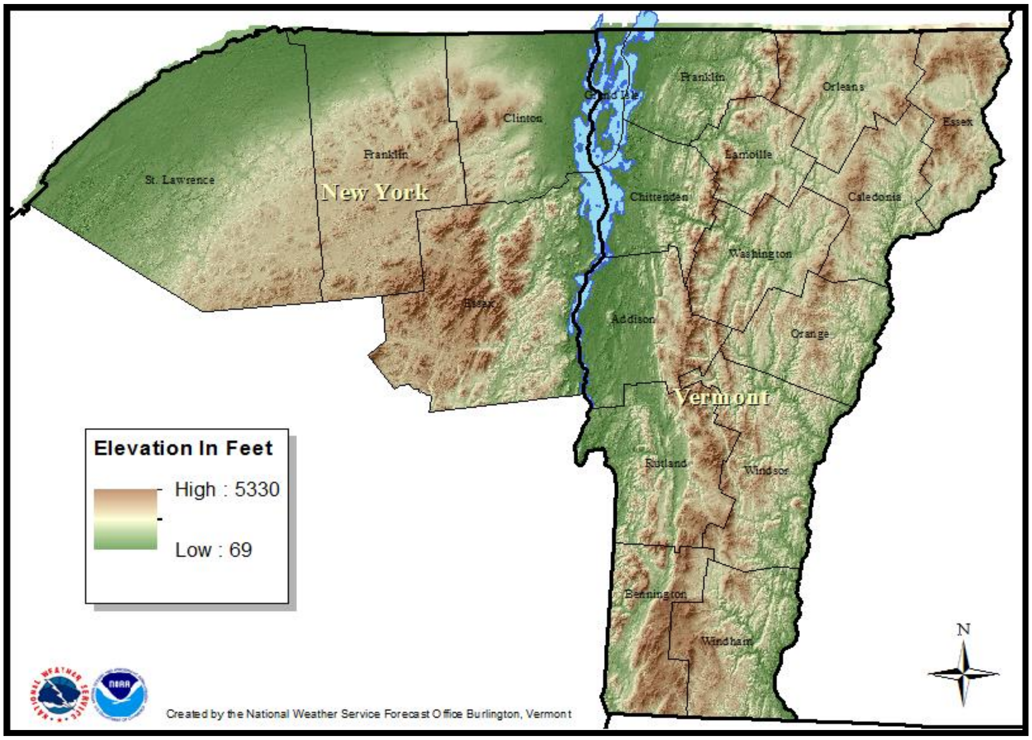

Figure 22. Plot of primary topographical features in the study area.